

# The MarkI helioseismic experiment.I. Measurements of the solar gravitational redshift (1976-2013)

T. Roca Cortés<sup>1,2</sup> and P. L. Pallé<sup>1,2\*</sup>

<sup>1</sup>*Instituto de Astrofísica de Canarias (IAC). E-38200, La Laguna. Tenerife. Spain*

<sup>2</sup>*Departamento de Astrofísica. Universidad de La Laguna (ULL). E-38206, La Laguna. Tenerife. Spain*

Accepted 2014 June 20. Received 2014 June 19; in original form 2014 February 21

## ABSTRACT

The resonant scattering solar spectrophotometer ‘Mark-I’, designed and build at the University of Birmingham (UK) and located at the Observatorio del Teide (Spain), has been continuously in operation for the past 38 years. During this period of time, it has provided high precision measurements of the radial velocity of the Sun as a star, which has enabled the study of the small velocity fluctuations produced by the solar oscillations and the characterization of their spectrum. So far, it has been one of the pioneer experiments in the field of helioseismology and contributed to the development of that area. Moreover, because of its high sensitivity and long term instrumental stability, it also provides an accurate determination (to within a few parts in  $10^3$ ) of the absolute daily velocity offset, which contains the so-called ‘solar gravitational red-shift’. In the present paper, results of the analysis of the measurements of this parameter over the whole period 1976–2013 are presented. The result of this series of measurements is  $600.4 \pm 0.8 \text{ m s}^{-1}$  with an amplitude variation of  $\pm 5 \text{ m s}^{-1}$ , which is in anticorrelation with the phase of the solar activity cycle. The 5% difference found respect to the value predicted by the equivalence principle is probably due to the asymmetry of the solar spectral line used.

**Key words:** general – helioseismology; sun, radial velocities; techniques.

## 1 INTRODUCTION

The redshift of spectral absorption lines from the solar photosphere has been known empirically since 1896 (Jewell 1896) and was then interpreted in terms of pressure shifts in the plasma of the solar photosphere. The formulation of the principle of equivalence and later of the General Theory of Relativity (Einstein 1911, 1916) indicated that this phenomenon was due to the difference in gravitational potentials between the solar photosphere and the Earth’s surface. This encouraged extensive observational work that has established with certainty that the solar redshifting of spectral lines is quite a complex phenomenon with the possibility of velocity fields, collisional effects, magnetic effects and other factors adding to the gravitational redshift (hereafter GRS) (Adam 1948; LoPresto, Kraus & Pierce 1994; Cacciani et al. 2006).

In contrast with astrophysical applications of the GRS, an experimental test became possible only after the discovery of the Mösbauer effect (Pound & Rebka 1960) and is undoubtedly capable of substantial improvement in the fu-

ture. Moreover, the use of atomic clocks (Vessot & Levine 1979; Vessot et al. 1980) has improved the accuracy of the measurements. There is no doubt that better clocks, as well as laser-based frequency standards, will make further improvements possible of the accuracy of measurements of the GRS on the Earth’s surface or in near-Earth space in the near future. Moreover, the use of laser-frequency combs is becoming a possibility for astronomical observations too (Steinmetz et al. 2008).

There has also been progress in our understanding of the conditions any theory has to satisfy in order to account for the GRS and also the implications of the existence of the GRS. These considerations show that a wide class of theories predict an identical GRS, and it is now appreciated that it is a rather weak test of relativistic theories of gravitation. However, Sciama (1964) points out that a measurement of the solar GRS, being over a distance very much greater than the scale height of the gravitational field is in principle preferable to local laboratory experiments and can test the validity of the minimum coupling principle.

In the final decades of the 20th century several measurements of the solar GRS were made using various techniques, such as improved solar spectrographs (Brault

\* E-mail: trc@iac.es; pere.l.palle@iac.es

1962; LoPresto, Schrader & Pierce 1991) and atomic beams (Isaak 1961; Snider 1970, 1972; Brookes 1974). The reported agreement with theoretical predictions for the strong resonance absorption lines of potassium and sodium, which are formed high in the photosphere, are within observational error of some 10%, including systematic effects. More recently (LoPresto, Kraus & Pierce 1994; Cacciani et al. 2006), there has been a better comprehension of the solar effects that add to the GRS, thereby reducing systematic errors and improving the results obtained.

Moreover, Brookes (1974), Brookes, Isaak & van der Raay (1976) and Fossat & Ricort (1973) introduced the use of alkali-vapour cells based resonant scattering spectrophotometers in the measurement of radial velocities in the Sun’s photosphere when observed as a star, resulting in an improvement of more than an order of magnitude over existing techniques (Jiménez et al. 1986). Works based on this technique, and some others, led to the discovery of solar oscillations and the birth of helioseismology. One such key instrument (Brookes, Isaak & van der Raay 1978), named MarkI, designed and built at the University of Birmingham (UK), has been in operation since 1975 at the Observatorio de El Teide (Canary Islands, Spain).

The dedication of this apparatus for such a longtime to solar observations has provided an enormous amount of valuable data and moreover, it served as a reference for other similar instrumentation build and operated later on, both in ground and in space. Now, with some historical perspective too, in a series of two papers we summarize the long standing observations and results achieved, we analyse the whole data obtained till now and report new findings and discoveries resulting from the precise measurements of the Doppler shifts of the 7699 Å resonance line of neutral potassium atom in the light integrated over the entire Sun (the sun viewed as any other star).

In this first paper, we briefly describe the apparatus, the observations achieved and the results of the analysis of its long-term time stability velocity signal which provided a long series of GRS measurements spanning from the years 1976 to 2013. In the second paper, a full in-depth description of the calibration of the data will be given and results of the analysis of the spectrum of the oscillations of the sun along three full solar activity cycles will be presented.

## 2 PRINCIPLE OF THE METHOD AND APPARATUS

The method used by resonant scattering spectrophotometry has already been described in detail (Brookes, Isaak & van der Raay 1978) and may be summarized here using Fig. 1 as a reference. Circularly polarized light with an absorption line, represented by the solid black curve, is incident on a suitable atomic vapour cell having a resonance line overlapping with the solar absorption line, placed in a longitudinal magnetic field of such strength as to locate the Zeeman components (blue and red curves) near the steepest parts of the solar absorption line. The intensity of resonantly scattered light due to left-handed circularly polarized incident light is given by  $L$ , whereas that due to right-handed circularly polarized light is given

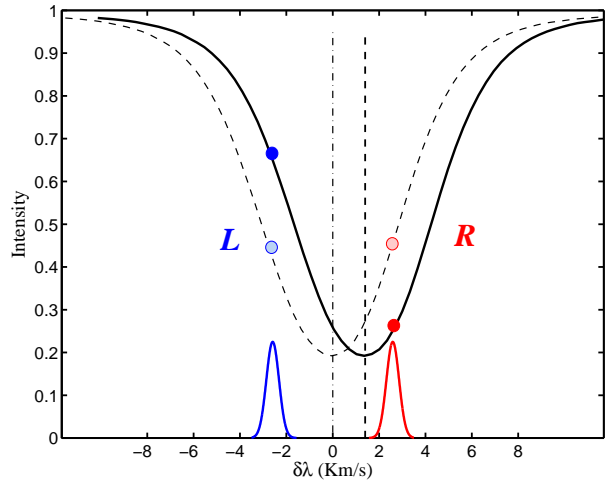


**Figure 1.** Principle of operation of the vapour cell resonant scattering spectrophotometry (see text). The relative displacement of the solar line with respect to the laboratory ones can be calculated by measuring at both wings (R and L) and making an appropriate ratio between both. In our case, observing integral sunlight with KI7699Å line, the dynamical range of the velocity shift spans from  $-300 \text{ m s}^{-1}$  (end September) to  $1500 \text{ m s}^{-1}$  (beginning April).

by  $R$ . It is clear from Fig. 1 that, when there is no relative displacement between the incident spectral line (dashed line) and the laboratory lines,  $L$  equals  $R$ . If, however, there is a relative shift between both lines, as illustrated in the figure (solid line), the two intensities are no longer equal, and the ratio defined as

$$r = \frac{L - R}{L + R} \propto V_{OBS} \quad (1)$$

gives a measure of the line shift corrected for intensity fluctuations to first order. Since the narrow laboratory Zeeman components scan the steepest parts of the broader solar line as the Earth spins, this method is extremely sensitive to very small shifts. In this experiment natural potassium vapour was used to study the relative position of the KI7699 Å absorption line with respect to the observatory. The solar line has a full width at half depth of  $6.23 \text{ km s}^{-1}$ , while the region probed by the laboratory lines is of order of  $1.8 \text{ km s}^{-1}$ , thus the ratio  $r$  will be almost linearly related to the velocity shift between the Sun and the laboratory to a first order approximation; in fact, a constant calibration of 3000 converts the ratio into velocity in  $\text{m s}^{-1}$  (van der Raay, Pallé & Roca Cortés 1986). A more detailed account of modifications due to the hyperfine structure and isotopic composition can be found in the more detailed and comprehensive paper (Brookes, Isaak & van der Raay 1978).

The MarkI apparatus, was developed and built at Birmingham University (UK) during 1973 and 1974, and was gradually improved over the following five years. A detailed account of its state during 1976 and 1977 in its first location in the *Casa Solar* at the Observatorio de El Teide (Tenerife, Spain) is to be found in Brookes, Isaak & van der Raay (1978) and Roca Cortés (1979). Briefly, a small, equatorially mounted servo-controlled heliostat (with flat mirrors)

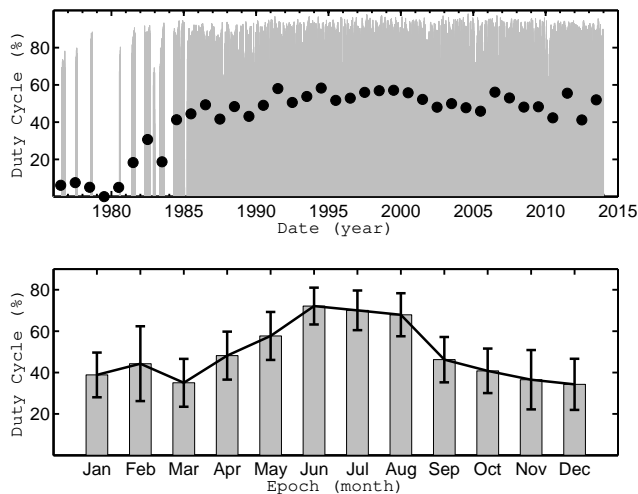


**Figure 2.** Top: duty cycle of daily MarkI solar observations throughout the years in percentage of daily useful hours (grey bars); the black dots are the annual values achieved in that year. Bottom: monthly averages (over the observed years) of the duty cycle with its standard deviations.

directs disc-integrated sunlight, suitably filtered by a thermostatically controlled interference filter centred at 7699 Å with a bandwidth of 15 Å, through a polarizer and an electro-optical light modulator, which alternately produces the required left- or right-handed circular polarization by the application of appropriate electric potential. The light then enters a vapour cell situated in a longitudinal field provided by a permanent magnet (0.18 T); the resonantly scattered light is then detected by a cooled photomultiplier tube (PMT), and the processed output pulses are recorded for subsequent computer analysis. In order to test for various optical and electronic asymmetries and to assess the overall stability of the system, a light source on its own or a white light (quartz-iodine) with a vapour cell in a transverse magnetic field to provide an artificial absorption line simulating the solar potassium line was also used.

### 3 OBSERVATIONAL PROCEDURE AND STRATEGY

From 1975 onwards, the MarkI instrument has been used exclusively to study the oscillations of the Sun as a star, and the measurement of the GRS is a byproduct that will be studied in this work. The one and only exception was in the 1979 summer campaign, in which the apparatus was used to look at different parts of the solar disc. Integrated sunlight helps to reduce the random shifts of the spectral line due to small scale motions in the solar photosphere. Moreover, it has the advantage that the rotation of the Sun is averaged to zero and possible instrumental errors due to imprecise guiding or atmospheric turbulence become minimized. Small signals due to angular non-uniformities on the photosphere, such as sunspots, or in sky transmission, or instrumental errors will be discussed later on.

MarkI was taken to the Observatorio de El Teide in 1975 and began operation by the end of that summer for only a few days. Several long summer observing campaigns were

then carried out there until 1984. During those years MarkI's performance was being monitored and used to develop other apparatus, based on the same principle, that helped to establish helioseismology as an astrophysical discipline in its own right. Moreover, from summer 1985 onwards, the observations were taken on a continuous daily basis in a fairly undisturbed and regular observational procedure. Its precise location at the observatory has been changed twice, the most recent being in 1986 when it was moved to its current location, the solar lab named *Pirámide van der Raay*. From 1993 onwards, it is also a node of the BiSON helioseismology network (Chaplin et al. 1996).

The sunlight enters the spectrophotometer through an open-air double flat mirror heliostat system. The two-axis servo-controlled primary mirror (which also moves along the north-south line throughout the year) feeds a fixed secondary mirror, which provides a horizontal sunlight beam towards the spectrophotometer room. This system, although symmetric about noon, has to be altered by changing the secondary mount at the equinoxes, otherwise it will cast shadow on to the primary around noon. Before 1979, the heliostat system was different and had an extra fixed flat mirror to accommodate the sunlight beam properly; also, the mirrors were of lower quality.

Minor changes in the core parts of the apparatus have been introduced, and it can be said that, up till 2009, MarkI has been working without interruption, weather permitting, other than a few failures that have been solved quite rapidly. The main changes have been in the electronic readout system that evolved from fast analogue electronics and seven-track magnetic tapes to fast digital electronics and a micro-computer system with cassette tapes in 1984; obviously, new computer hardware and software has been incorporated to the apparatus as it has become available and possible. Its performance has been outstandingly good; just recently, in October 2009, the vapour cell and PMT had to be changed because of darkening of the windows in the former and loss in efficiency in the latter, which lowered the count rate and signal-to-background ratio.

The raw data consist of a one-second measurement on the left-hand side of the line followed by a second on the right hand. The count in each channel usually spans from 0.1 to  $1 \times 10^6$  counts per second depending on sky transparency, thin cirrus and mirror cleanliness. Furthermore, the ratio is calculated by finding its average and standard deviation on the basis of blocks of 42 s (40 s from 1984 on), which, when calibrated to velocity, results in an error of  $\approx 1 \text{ m s}^{-1}$ .

The census of the observations during these years can be seen in Figure 2. Longer runs have been achieved in summer months when a higher number of daytime hours and cloudless days is more frequent; June, July and August are consistently the best months of the year. However, in winter the duty cycle is consistently lower even though the transparency of the sky is better; December and March are the months with the lowest duty cycle (around 40%). Note that, up to 1985, observations were taken only in summer-month campaigns. The duration of failures due to instrumental problems would be equivalent to a couple of useful days per year on average.

To summarize the amount of data in hand in a few numbers, it may be said that in the period from July 1976 to December 2013, with a total span of 13672 days, we have

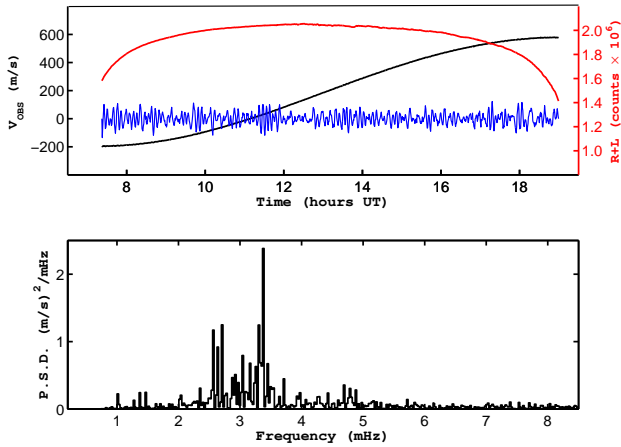


**Figure 3.** Results of a typical day's observing with MkI (2011 August 30). The top graph shows the following curves: observed velocity (in black), a hundred times the residuals after a sine wave fit (in blue) and the light transmitted (in red) through the apparatus. The bottom graph shows the power spectral density of the residuals with the 5 min solar oscillations being clearly seen above noise level.

observed for 8849 days. However, in the period from June 1984 to December 2013, where daily observations are available, out of a total span of 10958 days we obtained 8390 days of observations for a duty cycle of 49% of all possible daily hours.

Currently, the whole MarkI (level 1) database is accessible at the SVO site (Spanish Virtual Observatory <http://svo2.cab.inta-csic.es/vocats/marki>).

#### 4 DATA ANALYSIS

The result obtained on a typical day of observation is shown in Fig. 3 (top graph). If all the displacements of spectral lines of the Sun with respect to the laboratory are expressed in terms of relative velocity of the Sun with respect to the laboratory, at any given time we have:

$$V_{OBS} = V_{ORB} + V_{SPIN} + V_{GRS} + V_0 + V_{OSC} \quad (2)$$

where,

$$V_{ORB} = (\mathbf{V}_{\odot} - \mathbf{V}_{\oplus}) \cdot \mathbf{u}_r \quad (3)$$

is the resolved component of the relative velocity between the Sun and the Earth along the unit radius vector joining their centres, with due allowance for the planetary and lunar perturbations,

$$V_{SPIN} = \mathbf{V}_{rot\oplus} \cdot \mathbf{u}_r = \Omega_{\oplus} R_{\oplus} \cos \lambda_{obs} \cos \delta_{\odot} \sin \left[ \frac{\pi}{12} (t - t_0) \right] \quad (4)$$

is the component due to the observatory's daily rotation, where  $\Omega_{\oplus}$  is the angular velocity of the Earth,  $R_{\oplus}$  is the observer's distance from the centre of the Earth,  $\lambda_{obs}$  is the latitude of the observatory and  $\delta_{\odot}$  is the declination of the Sun and  $t_0$  is the local noon,

$$V_{GRS} = \frac{GM_{\odot}}{c} \left( \frac{1}{R_{\odot}} - \frac{1}{2 \cdot 1AU} \right) - \frac{GM_{\oplus}}{cR_{\oplus}} = 633.7 \text{ m s}^{-1} \quad (5)$$

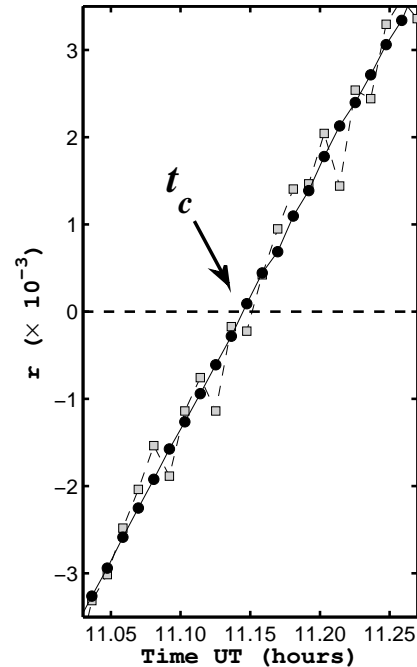
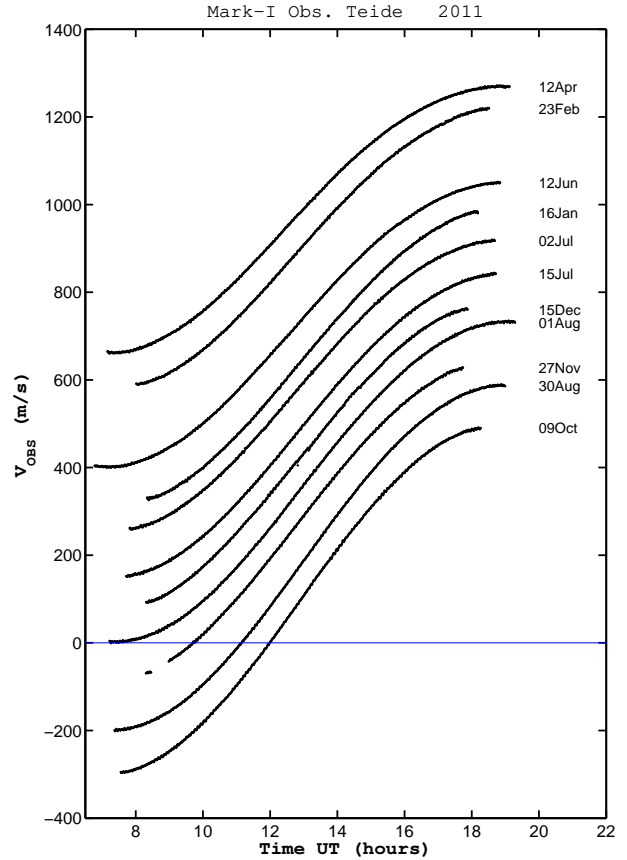


**Figure 4.** Top graph: a few days' observations spread over the year, illustrating that only around the interval spanning from the beginning of August to the beginning of December does the observed daily velocity curve cross the zero value. Bottom graph: zoom to show the obtaining of the crossing time,  $t_c$ ; that is, the precise time of the day when the velocity of the sun relative to the observatory is zero (on 2011 August 30).

is the GRS velocity equivalent (including the relativistic Doppler effect), where  $G$  is the gravitational constant,  $c$  the speed of light and  $M_{\odot}, R_{\odot}, M_{\oplus}, R_{\oplus}$  are the masses and radii of the Sun and Earth respectively, and

$$V_0 + V_{OSC}(t) \quad (6)$$

are unknown solar velocities; the first term representing the aperiodic solar velocity fields that can be considered stable over a day while the second stands for the measured global oscillations with periods lower than a day (Claverie et al. 1979).

Figure 3 shows the output of a typical day's observing, where the ratio  $r$  (in black, already calibrated in velocity), its residuals after a sine wave fit (multiplied by 100, in blue) and the transmitted light (in red) through the apparatus are shown; the bottom graph of Fig. 3 shows the power spectrum of the residuals of a fitted sine wave to the ratio/velocity curve, where the resulting solar five minute oscillations are clearly visible.

The term  $V_{GRS}$  is expected to be constant (over an Earth orbit it will only change by as much as  $0.1 \text{ cm s}^{-1}$ ),  $V_{ORB}$  varies along the year, from  $502 \text{ m s}^{-1}$  around April to  $-500 \text{ m s}^{-1}$  around October, with a maximum of  $\approx 12 \text{ m s}^{-1}$  between successive days, whereas the  $V_{SPIN}$  varies sinusoidally over a day with an amplitude that changes from  $375$  and  $408 \text{ m s}^{-1}$  at Observatorio de El Teide, depending on the Sun's declination. These terms can be better seen in Fig. 4 (top). Note that these Earth movements provide an accurate (and daily) calibration of the Doppler measurements in terms of velocity units to the nearest  $\text{cm s}^{-1}$ . On the other hand, instrumental, systematic and random noise can provide spurious velocity terms that will be dealt with further in this paper.

## 5 TWO METHODS TO MEASURE THE GRS

### 5.1 Null measurement method

The seasonal changes of the  $V_{obs}$  daily observations (due to  $V_{ORB}$ ) can also be clearly seen (Fig.4) and it can be noticed how the  $r$  ratio crosses zero value once at some time in the mornings of summer–autumn seasonal days. In fact, at Observatorio de El Teide it happens roughly from August 1 to December 1. At that precise time  $t_c$ , the solar absorption line and the laboratory line have a relative velocity zero shift. It is clear that such a null observation provides a very sensitive means of determining a daily value for  $V_{GRS} + V_0$  (see equation 2) in terms of the very accurately known value of  $V_{ORB} + V_{SPIN}$  at  $t_c$  (see Fig. 4, bottom) from the astronomical ephemerides. The term  $V_{OSC}(t)$  with the information of the solar oscillations is very small in amplitude ( $\approx 1 \text{ m s}^{-1}$ ), having low period signals (around 5 min); obviously, this signal can be filtered out quite well if need be. Moreover, this null measurement is independent of various background instrumental noise problems and curvature effects of the solar absorption line near the operating region, being independent of the calibration of the apparatus in terms of velocity, at least to first order.

Therefore, a way of obtaining the crossing time is to fit a straight line to the data on a given short time interval around the zero velocity crossing. The interval should be

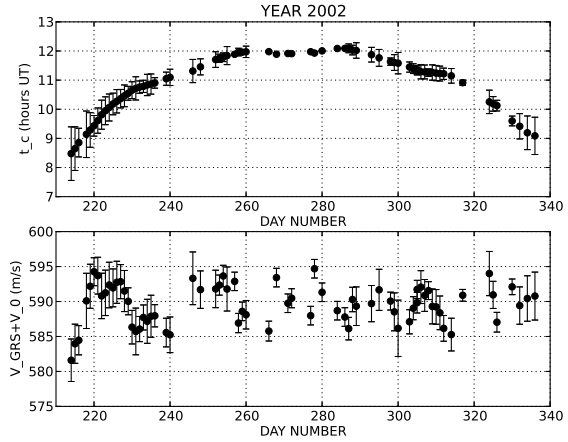


**Figure 5.** The GRS velocity obtained during any of the observed years. Top, the crossing time obtained from the observations (error bars are  $10 \sigma$ ) and, bottom, the corresponding calculated velocity with  $1\sigma$  error bars.

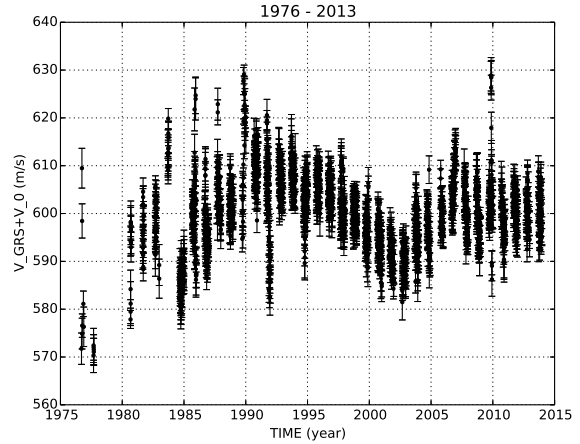


**Figure 6.** Raw values of the GRS velocity obtained during all years on the days where observations are available and the crossing time can be measured.

short enough so that a straight line is a good approximation and long enough so that the oscillation signal can be appropriately averaged out. The interval found to be appropriate is 40 min centred on the crossing time. The actual way of measuring the crossing time is shown in Fig. 4 (bottom); following the use of a moving mean filter, a straight line is fitted and the crossing time and its uncertainty calculated. The fit has been made with and without filtering; moreover, several appropriate filters were also checked without significant changes in the result.

For any one year of observation typically under 90 daily independent measurements are obtained that can be seen plotted in Fig. 5, where the crossing time over that season is shown in Fig. 5, where the crossing time over that season is shown in Fig. 5, while in the bottom graph the calculated  $V_0^{t_c} = V_{GRS} + V_0$  daily values are also plotted. It can be seen that the average value in that year,  $589.7 \pm 0.3 \text{ m s}^{-1}$ , is not the one expected from the first term alone; therefore,  $V_0$  is not null. Moreover, there are day-to-day variations well

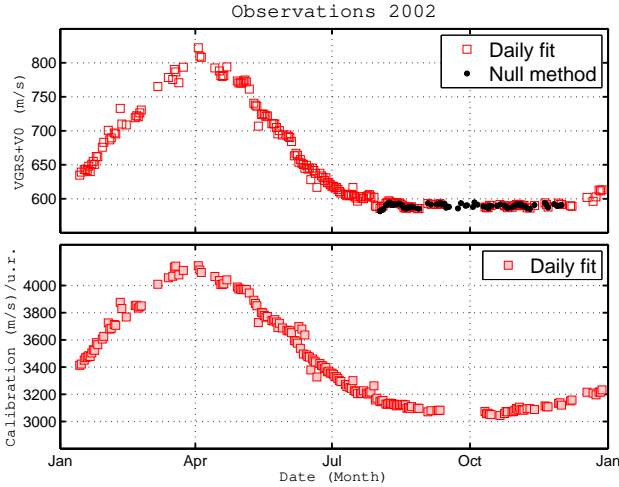


**Figure 7.** Results of the offset velocity ( $V_{GRS} + V_0$  and the calibration  $K$  obtained with the noon-measurement method for the year 2002. Notice the different behaviour around April from the one around October. Also plotted (black dots) is the result obtained with the first method (null measurement method) whenever available (August–November). Notice the different behaviour in April, where the most asymmetric parts of the line are sampled, from the one around October, where the parts sampled are symmetric.

outside the errors on each measurement. Such daily peak-to-peak variations, around  $10 \text{ m s}^{-1}$  and periods around half the solar rotation period (see Fig. 5), clearly suggest the activity features in the photosphere moving across the visible solar hemisphere. Therefore, we need to understand this result, which is rather similar in all years with observed data.

Moreover, these calculations are done over all the days of observation in which it is possible to obtain the crossing time and the results are plotted in Figure 6. In this figure the measurements show a mean value of  $601.14 \pm 0.15 \text{ m s}^{-1}$ , which is some  $32 \text{ m s}^{-1}$  lower than the predicted GRS velocity. Therefore, the  $V_0$  term will be non-zero owing to contributions from several sources, both solar and instrumental.

## 5.2 Measurement at noon method

A second method to daily measure the GRS would be to perform a measurement at noon time. As explained in section 4, notice that when  $t = t_0$  the term  $V_{SPIN} = 0$  and the equation 2 can be expressed as:

$$\begin{aligned} V_{GRS} + V_0 &= V_{OBS}(t_0) - V_{ORB}(t_0) - V_{OSC}(t_0) \\ &\approx V_{OBS}(t_0) - V_{ORB}(t_0) \end{aligned}$$

Therefore, a daily value for  $V_{GRS} + V_0$  can be obtained in terms of the known daily value of  $V_{ORB}$  (from the astronomical ephemeris) and the determination of  $V_{OBS}$  at  $t_0$ ; notice that  $V_{OSC}(t_0)$  is lower than  $1 \text{ m s}^{-1}$ . However, the determination of  $V_{OBS}(t_0)$  involves a process of calibration from the instrumental velocity (the observed ratio, see equation 1) to line-of-sight velocity in  $\text{m s}^{-1}$ . On the other hand, this method allows a daily measurement along the whole

year, provided the method of calibration is precise and stable enough. Although a full and precise description of the calibration procedure involving explanations and corrections of non-linear terms will be done in detail in the second paper of this series, we will provide here arguments that prove that under the best conditions (those very close to the linear regime) the results obtained for the GRS velocity coincide with the above explained null method.

A very simple and effective way of daily calibrating the measurements can be described as follows. From Fig.4 and equation 2, the measured ratio at any time can be expressed in the following way:

$$r(t) = a + b \sin \left[ \frac{\pi}{12} (t - t_0) \right] \quad (7)$$

Therefore, assuming a linear relation between ratio and velocity, this equation can be fit to the observations of any single day and obtain the daily values of the calibration  $K$  and the velocity offset ( $V_{GRS} + V_0$ ) as:

$$K = \frac{\Omega_{\oplus} R_{\oplus} \cos \lambda_{obs} \cos \delta_{\odot}}{b} \quad (8)$$

and

$$(V_{GRS} + V_0) = K \cdot a - V_{ORB}(t_0) \quad (9)$$

The results obtained for a typical year, say 2002, are shown in Fig.7. As it can be seen, from beginning of August to beginning of December is when the measurements are done under the most favourable conditions (when the most symmetric parts of the line are being sampled, see Fig.1) and both, calibration and velocity offset, are almost constant; notice that this is precisely the same epoch where the crossing time method (described above) can be applied. On the contrary, when measurements are done in the least favourable conditions, around April when the sampled parts on the wings of the line are asymmetric, the calibration changes by some 35% and the offset velocity also changes accordingly. It can also be noticed that in this later case the scatter of the points is higher than in the former. Notice also that the null measurement method, when applicable, coincides extremely well with those obtained with this method (the average of the differences is  $0.6 \pm 0.2 \text{ m s}^{-1}$ ).

In order to better calibrate the apparatus along the whole year it is necessary to linearise the measurements (to correct for the non-linearity of the line profile) in such a way that the results for the calibration become as constant as possible along the whole year. Although some methodology for very similar observations has been extensively described already in the past (see for instance (van der Raay, Pallé & Roca Cortés 1986; Pallé et al. 1993), in the next paper of this series it will be fully discussed.

## 6 INTERPRETATION AND CORRECTIONS

Figure 5 shows a clear daily variation with periods around half the solar rotation period, the so called 13-day period variation due to the passage of sunspots and other inhomogeneities across the visible solar photosphere, already pointed out in the past by Edmonds & Gough (1983), Durrant & Schröter (1983), Andersen & Maltby (1983) and Herrero, Jiménez & Roca Cortés (1984). Moreover, the  $V_0$

term will, or can, have contributions from many other sources, mainly solar but also instrumental. In this section we will try to understand such contributions.

### 6.1 Solar magnetic activity effects

The signal due to the passage of magnetic activity features over the visible solar hemisphere can be modelled by trying to match the observed data and can eventually be subtracted from observations. A simple model has been developed using the impressive sunspot data archive in NOAA-NGDC (<http://ngdc.noaa.gov/>), where daily sunspot areas and positions are recorded from well before our observations began up till now with very few gaps. The numerical model is fairly simple and has been used in slightly different ways in the past (see the above-mentioned authors). In this paper we have followed the work of Herrero, Jiménez & Roca Cortés (1984).

The numerical model simulates, at any point on the solar surface, all known line-of-sight relative velocities of the Sun with respect to Earth and the way the apparatus makes the measurement of the solar lines over the period of a year. Data on the potassium solar line, both in the quiet sun and in the sunspots, are taken from observations in the literature (Roca Cortés, Vázquez & Wöhl 1983; Bonet et al. 1988; Marmolino, Roberti & Severino 1987). All involved lines (solar and laboratory) are taken as gaussians, which is a good enough approximation for the scanning interval at work in the experiment. Moreover, it also includes the so-called limb-shift effect, which is caused by the granulation velocity fields present in the Sun's photosphere whose effect result in asymmetries in the spectral lines (the C-shapes bisectors), and change as we move from centre to limb (Dravins, Lindergren & Nordlund 1981; Dravins 1982; Roca Cortés, Vázquez & Wöhl 1983; LoPresto & Pierce 1985). As we observe the Sun as a star, the measurements will be affected by the disc-integrated result of this effect and for the KI7699Å line it has been measured in the past (Anguera et al. 1987; Andersen et al. 1985; LoPresto, Kraus & Pierce 1994) and studied theoretically by Marmolino, Roberti & Severino (1987), turning out to be small, with some differences among various authors. We have used an average value of the measured effect from the above mentioned authors, whose shift of the line is approximated by a second order polynomial in  $\mu$  ( $\mu = \cos \theta$ , where  $\theta$  is the heliocentric angle). Finally, it should be stated that the numerical model designed in this way has no free parameters.

The daily results for years 2002 and 2008 (high and low level magnetic activity years) are shown in Fig.8 where the GRS measurements obtained with the noon-measurement method (see subsection 5.2) are also shown for comparison. These simulated results are also calculated for every day at noon and are expressed in velocity using the daily calculated calibration from the model. As it can be seen, the numerical model follows very well the daily observations on both years, showing that the model seems to work well, even in both extreme conditions (the most favourable around October and the least favourable around April).

The difference between both years (different level of solar activity) is in the average value of the observations ( $601.5 \text{ m s}^{-1}$  and  $590.3 \text{ m s}^{-1}$  for 2008 and 2002 respectively).

Also, the annually averaged values of the simulated data show a slight difference between both years, being of  $0.1 \text{ m s}^{-1}$  higher in 2008; other years with the highest activity only showed  $1.5 \text{ m s}^{-1}$  less than the lowest minimum. The offset velocity between model and observations is of some 50 to  $60 \text{ m s}^{-1}$ ; in order to obtain simulated values of GRS close to the ones observed we have to use a value for  $V_{GRS}$  of  $585 \text{ m s}^{-1}$  instead the one theoretically predicted (see section 4) or to modify the limb-shift effect. On the other hand, in Fig.8 the relative difference between model and observations is also plotted (mean value is subtracted). It is interesting to notice that the flat part of the curve, from August to November, is better fitted than the rest of the year where a higher scatter (more than a factor of two) and some slight curvature is left over. This is very probably due to the fact that in the measuring conditions around April the approximation of the spectral lines by gaussians is not good enough and it would need a better treatment.

Therefore, in what follows, we will concentrate in the observations made with the null-measurement method which, by definition, are done in the most favourable conditions, do not depend on the calibration of the measurements and, anyway, they coincide very well with the noon-measurement method (see Fig.7).

When the numerical simulation is applied to predict the GRS measurements at the crossing time (null-measurement method), the results found can be seen in Fig. 9 for the same years than before (2002 and 2008). The bottom graph shows the crossing time, obtained using the same procedure as the one used for the observations, where a small variation, with a period of nearly a month, can be clearly seen, due to the residual effect of the Moon on the Earth's orbit. The top graph shows the result of the GRS velocity variations for both years. Notice that, at solar activity minimum, the variation is negligible being well below  $1 \text{ m s}^{-1}$  while at maximum activity a signal of up to  $\approx 8 \text{ m s}^{-1}$  peak to peak variation is seen.

In this case, the comparison of the numerically simulated results with observations can be seen for the same years in Figure 10. The match is very good in 2002 given the observational errors, with the exception of certain details. For instance, the amplitude of the simulated signal is somewhat smaller than the observed one even though they both follow the same trends. In some other years, the simulated signal seems sometimes to lead the observed one (as already pointed out in (Herrero, Jiménez & Roca Cortés 1984)). These details would suggest that more realism in the simulation would be interesting and necessary, with the inclusion of the contribution from faculae, for instance, but this would be difficult owing to the lack of sufficient observational data for these features. Moreover, the inclusion of a better approximation of the line profiles (solar and lab) would probably help to obtain a closer match of the amplitudes. In Fig.11 and Fig.12 the results obtained for the years 1984 to 2013 are shown. Observations prior to 1984 were only limited summer campaigns and were performed with different heliostat system and readout electronics (see section 3).

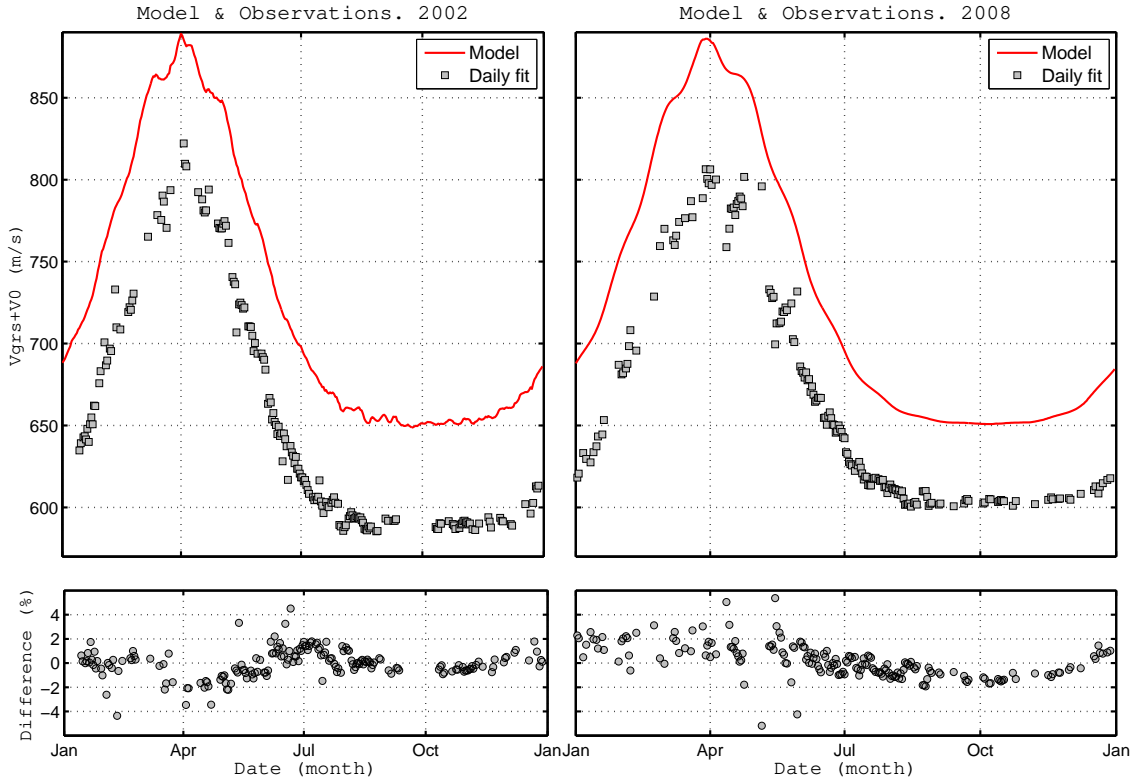


**Figure 8.** Top, results from the numerical model for two years with high (2002) and low (2008) magnetic activity and its comparison to observations analysed with the noon-measurement method. Bottom, the relative difference is plotted after being subtracted its mean value, showing a good match and less scatter in the August to November epoch.

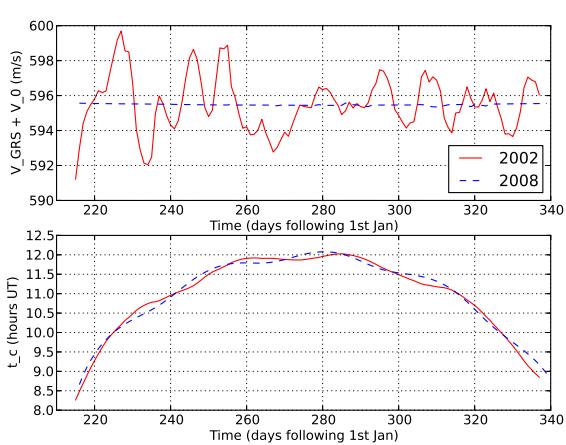


**Figure 9.** Results from the numerical model (see text) for years 2002 (near maximum solar activity) and 2008 (near minimum solar activity). Top graph shows the GRS velocity obtained using the same procedure as the one used with the observations, while on the bottom graph the crossing time is shown. Both parameters are obtained with the same procedure applied to the observed data (see section 5.1).

## 6.2 Instrumental systematic errors

A thorough analysis of the possible instrumental errors in the apparatus is to be found in Brookes, Isaak & van der Raay (1978) and in Roca Cortés

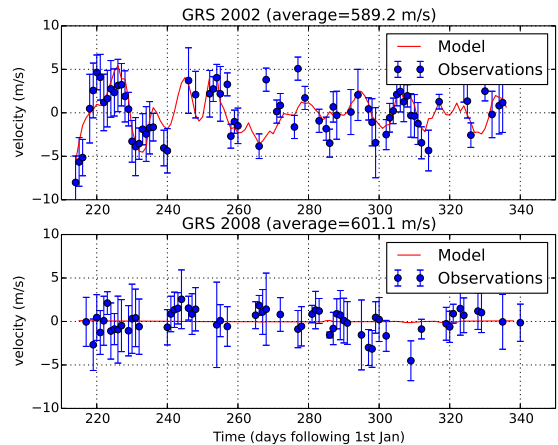


**Figure 10.** Comparison of the GRS velocity results obtained from observations (blue dots) and the results of the numerical simulation (red line) in a year close to solar activity maximum (2002, top) and for another close to minimum solar activity (2008, bottom).

(1979). During the observing days many tests have been done that confirm the expected results of these analyses. Such tests were always performed by changing one parameter at a time and leaving at least a complete day of observation to be able to measure the potential effect of the change on the observed data. Moreover, from 1985 onwards,



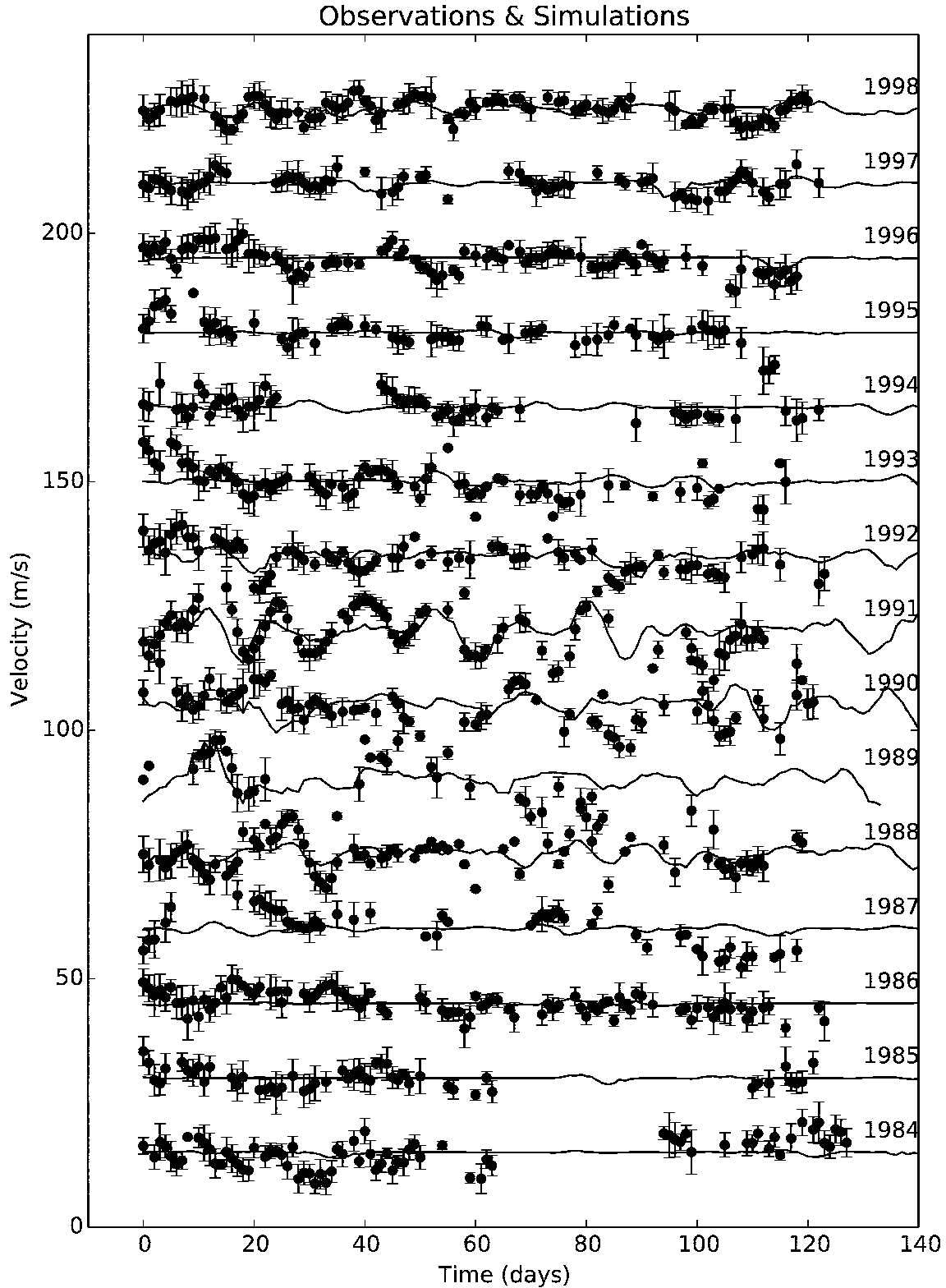


**Figure 11.** Comparison of the observations and the results obtained from the numerical model described in the text. The graph shows the annual observed GRS velocity (with its average subtracted) and the results obtained from the numerical model. For clarity, the vertical scale is built by adding 15 m/s to previous years' results. The first day plotted is the first day of that year with null-method measurements.

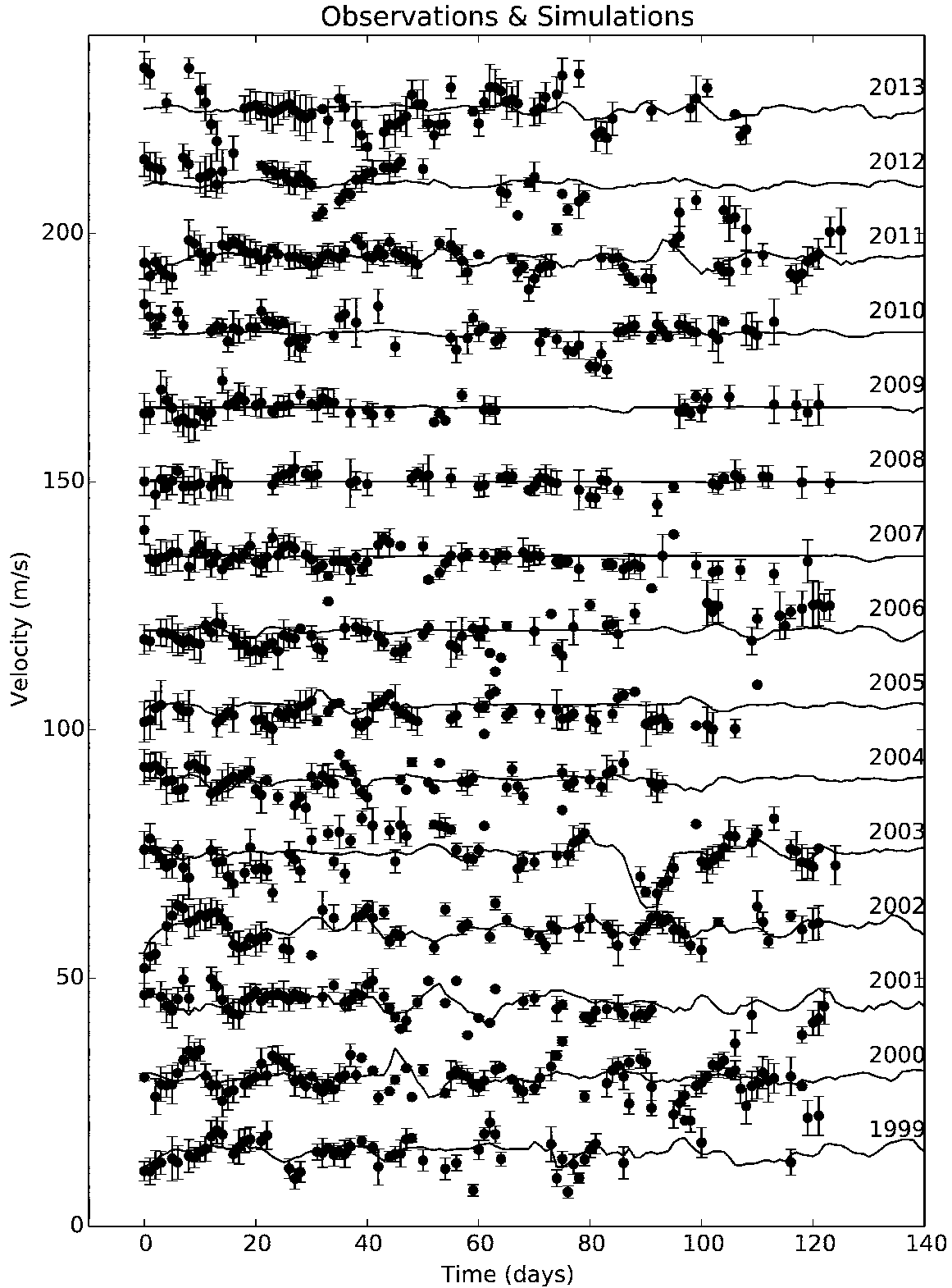


**Figure 12.** Comparison of the observations and the results obtained from the numerical model described in the text. The graph shows the annual observed GRS velocity (with its average subtracted) and the results obtained from the numerical model. For clarity, the vertical scale is built by adding 15 m/s to previous years' results. The first day plotted is the first day of that year with null-method measurements.

some housekeeping data, such as temperatures at different points of the spectrophotometer (always kept below 1K fluctuations) and guiding errors, have also been recorded. These are very small, for an integration time of 40 seconds the error is  $1.8 \pm 0.6$  arcsec and it is below 0.1 arcsec for any given day. The pointing sensitivity has been measured to be less than  $0.8 \text{ m s}^{-1}/\text{arcmin}$ .

To summarize the results here, it can be said that the systematic errors (mechanical, thermal, optical and electronic) are kept well below the  $1 \text{ m s}^{-1}$  level in all parts of the instrument. Possible electronic asymmetry between both channels (L and R) and long term instrumental stability were checked in dedicated long runs using appropriate calibration set-ups; all tests have shown uncertainties of  $\approx \pm 0.1 \text{ m s}^{-1}$ . Moreover, the magnetic field of the permanent magnet showed no significant change over the years. However, the most sensitive source of error is misalignment of the electro-optical light modulator (EOLM) with respect to the entrance beam. This can happen near the equinoxes, when the secondary mirror mounting has to be changed. This is a major change and the alignment is checked, a realignment usually being required; however, the same relative position between the entrance beam and the EOLM axis is sometimes not achieved, resulting in a slight change in the offset velocity. The resulting effect on the daily offset velocity measurement is illustrated in Fig. 13 with an example; in the graph, the day of the mount changeover is shown by a green vertical line, and a step in the measured velocity can be seen. By calculating the mean value of a few points before and after the mount changeover we can correct for such systematic effects.

Another systematic effect might come from the existence of the isotope  $^{41}\text{K}$  with a proportion of 7.4% respect to  $^{39}\text{K}$  which produces an isotopic shift of up to  $-98 \text{ m s}^{-1}$  as the optical thickness of the vapour changes from thin to thick (Jackson & Kuhn 1938). These effects will be measurable if the optical thickness of the gas is different in the cell from that on the Sun's atmosphere, or if it changes with time. Moreover, while there is no reason for a significant change in optical thickness on the Sun, in the cell it can change only if the temperature of the oven heating the cell changes. This parameter has been measured (every minute) and recorded from 1985 onwards; it is found to vary very smoothly during the day typically by  $\pm 1$  degree (which represents 0.7%) owing to room temperature variations. The same cell was used from 1976 to 2009; in the years 1977, 1985 and 2000 tests were performed by carefully changing the setting of the oven voltage heating circuit by an amount as high as 10% (in power), with very small effects of less than  $0.5 \text{ m s}^{-1}/\%$  being found in the results.

## 7 DISCUSSION OF THE RESULTS

Once the numerically calculated effect of the passage of the sunspots is corrected, yearly averages of the GRS velocity are obtained; these are plotted in Figure 14. As can be seen, there are some points that diverge considerably from the mean value such as those obtained during the first three years; data from 1976 to 1978 result some 25 to  $30 \text{ m s}^{-1}$  lower than the rest. This is interpreted as an instrumental effect brought about by the fact that, in these years,

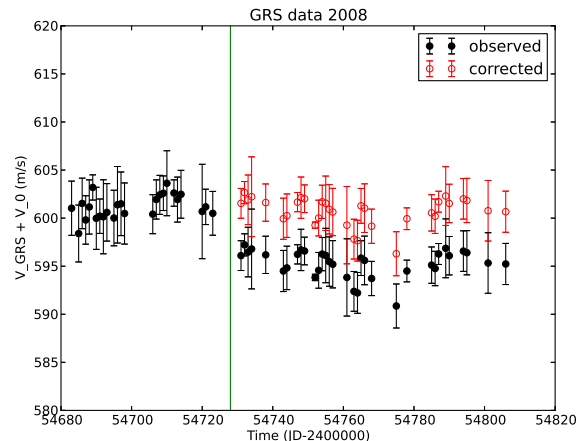


**Figure 13.** Instrumental effect on the observed GRS velocity due to the summer to winter secondary mirror mount changeover (a green vertical line shows the precise day) and the corresponding re-alignment. Notice that if a positive shift is added to the black dot points following the mount changeover's day to obtain the red open circle points, the observed velocity now shows a nice continuity with the observations obtained before.

the heliostat system that feeds the spectrophotometer with the incident beam was different (the primary was displaced from the north–south line defined by the secondary and had to be changed at noon) from that used afterwards and included mirrors of much lower quality. Moreover, in 1983 we had very few useful results (as much as six) as the electronic channel analyser in the data collection system did not work properly and had to be replaced. These points have therefore been disregarded. Finally, in the years 1990 to 1993, the systematic effect in the secondary mount changeover was kept  $14 \text{ m s}^{-1}$  too high. Once these considerations were taken into account and the data points were corrected, a second definitive graph (see black dots in Fig. 14) was produced.

These changes have been considered in the data and the final average found is  $600.38 \pm 0.78 \text{ m s}^{-1}$ , which corresponds to  $94.75 \pm 0.1 \%$  of the full effect predicted by the principle of equivalence. Note that the statistical error is the lowest ever measured on the Sun. However, it also shows a variation of  $\approx \pm 5 \text{ m s}^{-1}$  with a period of 10–12 years, which is very close to the solar activity cycle's mean periodicity. In order to understand this effect we have plotted, in Fig. 15, the results found, together with an average of the international sunspot number over the same days where we had GRS data, taken from (SIDC 2014) (<http://sidc.oma.be/sunspot-data/>). A clear anti-correlation can be seen between the two graphs, suggesting an explanation in terms of magnetic activity influencing the symmetry of the solar line profile.

Such a 5% difference from the predicted GRS value can be explained as follows. The only instrumental error that can account for such difference is that in the optical depth of the potassium atoms in the Sun rather than in the cell; if this were so, the differential isotopic shift could explain the difference. However, in our opinion, this is not the most plausible explanation. The solar line is a strong resonance line that is optically thick in the Sun. In the laboratory the vapour cell, in the MarkI apparatus, the optical depth de-

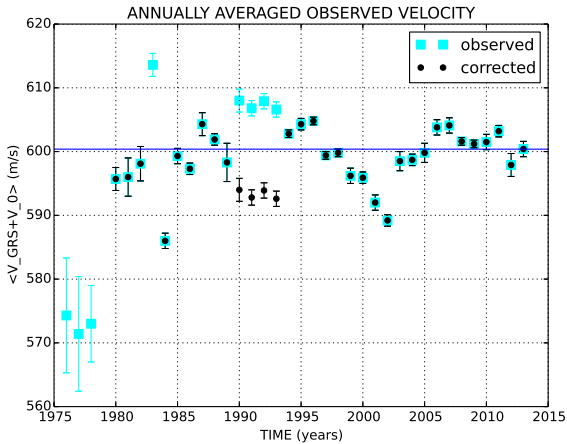


**Figure 14.** Yearly averages of the observed velocities (cyan squares) following the subtraction of the solar activity effect on the measurements. In black circles, the same data once some values (1990–93) for instrumental systematic errors are corrected and others (1976–1978,1983) due to different heliostat set-up (see text) are removed.

depends on the number of atoms present in its head, which is a consequence of the temperature at which the cell is being heated. The voltage in the oven is supplied by a very stable power supply that heats the cell up to 360 K; the oven voltage is measured with a thermistor, which shows that the temperature is kept stable close to 0.1 K during observations. The temperature is set so that a plateau in the scattered intensity is achieved; in these conditions the vapour is optically thick in the cell’s head. However, Snider (1974) in a research note reports the measurement of  $16.4 \pm 1$  mÅ, which corresponds to  $638 \pm 39$  m s<sup>-1</sup> using a potassium-based atomic beam resonant scattering spectrometer. Given that the error is much higher than ours, the difference in the value found here can be explained because in our case we are measuring integral sunlight rather than using a small aperture in the centre of the Sun’s image, therefore using a differently averaged solar potassium line profile and also a differently averaged solar limb shift effect.

The limb shift effect of this solar line, and the GRS itself, have also been measured by LoPresto, Kraus & Pierce (1994) at the Mac Math-Pierce solar telescope also using a small aperture on a large solar image. They also measured  $99 \pm 7$  % of the full predicted GRS value and a small linear limb shift. Another measurement of this effect has also been made by Andersen et al. (1985), who found a non-linear limb shift increasing rapidly when approaching the solar limb. The difference between both seems to be in the amount of scattered light from the centre of the Sun in the measurements at positions approaching the limb; in both works, the position of the solar line is determined by appropriately fitting its minimum. A third measurement came from our own group (Anguera et al. 1987), which found an intermediate result. Moreover, in our numerical simulation (see subsection 6.1) we find that the effect averaged over the whole Sun is  $\approx 15$  m s<sup>-1</sup>.

The resonant scattering experiments measure the solar line in its wings rather than by finding the minimum. Therefore, if the line is not symmetric the mea-

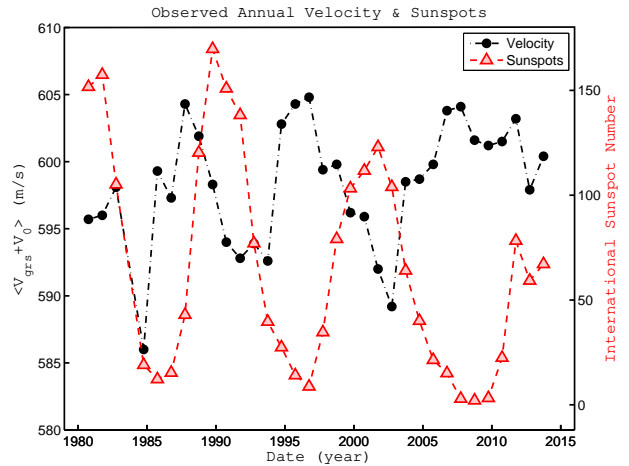


**Figure 15.** Final yearly averages of the GRS observed velocity (dots) and averages of the international sunspot number (triangles) calculated over the same time interval than the observations.

surement can be either blue- or redshifted with respect to the minimum. Measurements of the asymmetry of the KI7699 Å line made by LoPresto, Kraus & Pierce (1994) and Bonet et al. (1988) show that, at between 30 and 60% of the residual intensity, it is blueshifted at the centre of the Sun, while close to the limb it is centred or even redshifted with respect to the minimum. Using integral sunlight, Roca Cortés, Vázquez & Wöhl (1983) find that the wings are blueshifted by  $\approx 50 \pm 30$  m s<sup>-1</sup> with respect to the minimum. Very similar results are obtained if we analyze the data on the KI7699Å line from the integral sunlight atlas taken at Kitt Peak (Kurucz et al. 1984).

Taking such considerations into account, we believe this latter explanation, asymmetry of the solar line ( $-50$  m s<sup>-1</sup>) plus residual limb shift effect ( $15$  m s<sup>-1</sup>), explains the average GRS measured value.

## 8 CONCLUSIONS

The solar gravitational redshift measured in the KI7699 Å line for the years 1976 to 2013 has been obtained as a by-product of the measurements of solar oscillations taken on integral sunlight at Observatorio de El Teide, from 1976 to 2013, using the resonant scattering spectrometer MarkI.

The average result over this period results in  $600.4 \pm 0.8$  m s<sup>-1</sup>, with a clear variation, which is in anti-correlation with the phase of the solar activity cycle, of roughly  $\pm 5$  m s<sup>-1</sup>. Although the statistical error bar is the lowest ever measured, correction for this effect should bring it even lower. These measurements are amongst the most precise ever made of the solar gravitational redshift and the most numerous.

The value found for the GRS is  $33$  m s<sup>-1</sup> lower than the theoretically value expected (5% of the full effect). We believe that, besides considerations already taken into account, the anti-correlation found between the variations around the mean value and the solar activity cycle also suggest that the discrepancy can be attributed to the overall asymmetry of the Sun-integrated KI7699Å spectral line changing with magnetic activity.

An obvious consequence that can also be derived is that, when the radial velocities of other stars are studied, the currently reported findings warn against interpretations such as possible planets or other components orbiting around them, without first checking for stellar magnetic activity effects.

To improve this result it would be very convenient to avoid the use of solar magnetic sensitive lines. Moreover, the use of integral sunlight prevents observational problems, such as diffuse light, specially when measuring near the limb. However, the determination of the overall effect on integral sunlight of the convective limb-shift, in order to properly correct the measurements, is a very difficult task. Therefore, the use of spectral lines with small limb-shift would also be advisable.

## ACKNOWLEDGMENTS

The data used in this work, their temporal coverage spanning almost 40 years (an astronomer's lifetime), their continuity and quality, have involved the contribution of many individuals who developed and maintained the apparatus, the site where it stands and performed the observations, and also the support of several governmental funding institutions from Spain and the UK. It all started forty years ago, through a collaboration between the HiRES group at the Physics Department of the University of Birmingham (UB, UK) and the solar section of the Instituto Universitario de Astrofísica at the Universidad de La Laguna (ULL, Spain). We remain deeply indebted to all the individuals who made it possible.

However, this paper is dedicated to the memory of our friends and colleagues, the late Bill Brookes, George Isaak and Bob van der Raay (and their families) from the University of Birmingham (UB), actual designers, builders and early sustainers of the MarkI spectrophotometer apparatus. Also to the memory of the late Joan Casanovas (who began the collaboration), Montse Anguera and Irene González from the Instituto de Astrofísica de Canarias (IAC). One more detail is that the topic of this paper was first suggested and encouraged by Prof. G. R. Isaak.

We are also thankful to our technical colleagues who took care of updates and the main repairs of the instrument: Clive McLeod, Brek Miller and Steven Hale (and the late Joe Litherland) at UB and, Ezequiel Ballesteros and Andrew Jones at the IAC. Special mention of the maintenance team of the Observatorio del Teide (IAC) led by Ignacio del Rosario and the administrative and supportive personnel lead by Miquel Serra. We also thank the personnel of the Servicios Informáticos Comunes (SIC) of the IAC. The MarkI instrument manpower requirements at the beginning and the end of each daily observing run implies the need for observers at the site. Over the past 40 years, many people, nearly 100, have performed the observations: our colleagues and staff scientists of the IAC, summer students at the IAC, undergraduate students from the Faculty of Physics at the ULL and, recently, the team of observers at the Observatorio del Teide, coordinated by Alex Oscoz. We acknowledge their diligence and dedication. Many thanks to Lluís Tomás, Ricard Casas, Santiago López and particularly to Antonio Pimienta, who has been for more than twenty years (still he is) the 'curator' of the instrument and of its environment at the lab.

Staff scientists of the IAC's Helioseismology group have played a crucial role in the Mark-I data scientific exploitation, as most of them began their scientific career with it: Juan C. Pérez, Gary Bramford, Clara Régulo, Antonio Jiménez, Fernando Pérez, Stuart Jefferies, Luis Sánchez, Jesús Patrón, Isabel Martín, Antonio Eff-Darwich, Rafa García, Chano Jiménez and other colleagues that helped with the observations. Other institutions at the site, like KIS (Kieppenheuer Institut für Sonnenphysik) al-

ways helped aluminizing the mirrors. We are also indebted to Manuel Vázquez, the former leader of the incipient Solar Physics group at the IAC, for his continuous support. The Mark-I spectrophotometer became in the mid-nineties a node of the BiSON project (Birmingham Solar Oscillation Network), which consisted of another four nodes under the responsibility of Prof. Yvonne Elsworth (UB).

Institutional support have provided the services and funding necessary to ensure the continuity of MarkI observations: we thank the UB and the IAC for providing so many services (administration, electronic and mechanical workshops amongst others) over the entire operational period of the Mark-I. The Spanish Government, under different funding schemes that evolved during these years (currently the Spanish National Plan of Research and Development under grant AYA2012-17803), and British institutions (SERC at the beginning, then PPARC and, at present, the STFC, Science and Technology Facilities Council) have supported the MarkI project and later the whole BiSON network. Currently, the whole MarkI database is accessible at the SVO site (Spanish Virtual Observatory <http://svo2.cab.inta-csic.es/vocats/marki>); this initiative was developed in the framework of the FP7-SPACE-2011-1, project n.312844 (SPACEINN).

## REFERENCES

- Adam M.G., 1948, MNRAS, 108, 446  
 Andersen B.N., Maltby P., 1983, Nature, 302, 808  
 Andersen B.N., Barth S., Hansteen V., Leifsen T., Lilje P.B., Vikanes F., 1985, Sol. Phys., 99, 17  
 Anguera M., Pallé P.L., Régulo C., Roca Cortés T., Isaak G. R., McLeod C.P., van der Raay H.B., 1987, in Schröter E.H., Vázquez M., Wyller A. eds. The role of fine scale magnetic fields in the structure of the solar atmosphere, Camb. Univ. Press, p. 24  
 Bonet J.A., Márquez I., Vázquez M., Wöhl H., 1988, A&A, 198, 322  
 Braut T., 1962, Ph.D. Thesis, Princeton University, USA.  
 Brookes J.R., 1974, Ph.D. Thesis, University of Birmingham, UK.  
 Brookes J. R., Isaak G. R., van der Raay H. B., 1976, Nature, 259, 92  
 Brookes J.R., Isaak G.R., van der Raay H.B., 1978, MNRAS, 185, 1  
 Cacciani A., Briguglio R., Massa F., Rapex P., 2006, Cel. Mech. & Din. Astron., 95, 426  
 Chaplin W.J., Elsworth Y., Howe R., Isaak G.R., McLeod C.P., Miller B.A., van der Raay H.B., Wheeler S.J., New R., 1996, Sol. Phys., 168, 1  
 Claverie A., Isaak G.R., McLeod C.P., van der Raay H.B., Roca Cortés T., 1979, Nature, 282, 591  
 Dravins D., Lindegren L., Nordlund Å, 1981, A&A, 96, 345  
 Dravins D., 1982, ARA&A., 20, 61  
 Durrant C.J., Schröter E. H., 1983, Nature, 301, 589  
 Edmonds M.G., Gough D.O., 1983, Nature, 302, 810  
 Einstein A., 1911, Ann. Phys., 35, 898  
 Einstein A., 1916, Ann. Phys., 49, 769  
 Fossat E., Ricort G., 1973, Sol. Phys., 28 (2), 311  
 Isaak G. R., 1961, Nature, 189, 373  
 Herrero A., Jiménez R., Roca Cortés T., 1984, Mem. Soc. Astron. Ital., 55, 331  
 Jewell L.E., 1896, ApJ, 3, 89  
 Jackson D.A., Kuhn H., 1938, Proc. Roy. Soc, A165, 303  
 Jiménez A., Pallé P. L., Régulo C., Roca Cortés T., Isaak G. R., 1986, Adv. Space Res., 6 (8), 89.  
 Kurucz R.L., Furenlid I., Brault J., Testerman L., 1984, Solar Flux Atlas from 296 to 1300nm. Harvard Univ. Press  
 LoPresto J.C., Pierce A.K., 1985, Sol. Phys., 102, 21

- LoPresto J.C., Schrader C., Pierce A.K., 1991, *ApJ*, 376, 757L  
LoPresto J.C., Kraus P.M., Pierce A.K., 1994, *Solar Phys.*, 149, 243  
Marmolino C., Roberti G., Severino G., 1987, *Sol. Phys.*, 108, 21  
Pallé P. L., Fossat E., Régulo C., Loudagh S., Schmider F. X., Ehgamberdiev S., Gelly B., Grec G., Khalikov, S., Lazrek, M., 1993, *A&A*, 280, 324  
Pound R.V., Rebka G.A., 1960, *Phys. Rev. Lett.*, 4, 337  
van der Raay H.B., Pallé P.L., Roca Cortés T., 1986, in D.O. Gough ed *Seismology of the Sun and distant stars*, D. Reidel Pub. Co., p. 333  
Roca Cortés T., 1979, Ph.D. Thesis, Universidad de La Laguna, Spain  
Roca Cortés T., Vázquez M., Wöhl H., 1983, *Sol. Phys.*, 81, 1  
Sciama D.W., 1964, *Rev. Mod. Phys.*, 36, 463  
SIDC-team, World Data Center for the Sunspot Index, Royal Observatory of Belgium, Monthly Report on the International Sunspot Number, online catalogue of the sunspot index: <http://www.sidc.be/sunspot-data/>, 1980-2013  
Snider J.L., 1970, *Solar Phys.*, 12, 352  
Snider J.L., 1972, *Phys. Rev. Lett.*, 28, 853  
Snider J.L., 1974, *Sol. Phys.*, 36, 233  
Steinmetz T., Wilken T., Araujo-hauck C., Holzwarth R., Häusch T.W., Pasquini L., Manescau A., D'Odorico S., Murphy M.T., Kentischer T., Schmidt W., Udem Th., 2008, *Sci.*, 321, 1335  
Vessot R.F.C., Levine M.W., 1979, *Gen. Rel. Grav.*, 10 (3), 181  
Vessot R.F.C., Levine M.W., Mattison E.M., Blomberg E.L., Hoffman T.E., Nystrom G.U., Farrel B.F. Decher R., Eby P.B., Baugher C.R., Watts J.W., Teuber D.L., Wills F.D., 1980 *Phys. Rev. Lett.*, 45 (26), 2081